

# Technology of Closed-Drift Thrusters

Harold R. Kaufman

*Front Range Research, Fort Collins, Colorado*

## Introduction

A CLOSED-drift thruster is defined herein as a thruster in which ions are electrostatically accelerated in essentially the thrust direction, with the accelerating electric field established by an electron current interacting with a transverse magnetic field. One component of the electron motion is counter to the ion flow. Another component is normal to that direction. The current associated with this normal component is called the Hall current. In a closed-drift accelerator there is a complete, or closed, path for the Hall current. In addition, for the ions to be accelerated in essentially a single thrust direction, the ion cyclotron radius must be much larger than the total acceleration length.

Closed-drift thrusters usually employ axially symmetric electrodes and pole pieces, with the magnetic field in the radial direction and the electric field in the axial direction. The Hall current flows in a circular closed path in such a configuration. A few closed-drift thrusters without axial symmetry have also been investigated.

The closed-drift thruster is particularly well suited for operation in the 1000-2000 s range of specific impulse (approximately 10,000-20,000 m/s exhaust velocity). It is difficult to operate above about 1000 s with an electrothermal thruster due to excessive excitation and ionization losses. On the other hand, the space-charge-flow limitations of gridded electrostatic thrusters will not permit practical ion current densities below about 2000 s.

Within the 1000-2000 s range, the electron backflow required to establish ion acceleration can, for the most part, be used to generate ions. The generation of ions constitutes the major closed-drift thruster loss in this range of specific impulse, and this loss can be under 100 eV per beam ion.

The power processing requirements are also moderate. In a properly designed closed-drift thruster only one power circuit is required for steady-state operation, with the voltage of this circuit typically in the 50-500 V range.

## Historical Development

Most of the early closed-drift thrusters had dielectric channel walls and a channel length at least equal to the channel width, as indicated in Fig. 1.<sup>1-7</sup> In addition, the electron cyclotron orbit was small compared to the ac-

celeration length. The ion production was by either a contact-ionization process or an electron-bombardment volume-production process. This closed-drift thruster was called a Hall current type.<sup>1,4-7</sup>

During this early period another variation of closed-drift thruster was also studied, in which the length of the acceleration channel was considerably less than the channel width.<sup>8,9</sup> The acceleration in this type of thruster was believed to take place over a distance of the order of the local electron-cyclotron orbit. This closed-drift thruster was called a space-charge-sheath type.

The initial hope was that the electron current required to establish the accelerating electric field would be governed by classical diffusion. It was soon established that these axial electron currents were orders of magnitude above the classical value, presumably due to the turbulence, or oscillations, involved in the acceleration process.<sup>5</sup>

The range of interest for specific impulse in electric primary propulsion was 5000-10,000 s during the 1960-70 period. The electron backflow at these high specific impulses was energetic enough that it was difficult to use efficiently in volume ion production. The large electron backflow therefore constituted a major loss. It is true that this electron backflow could have been used to heat the ionizer of a contact-ionization thruster. But contact ionization had other problems, including excessive heating-power requirements and difficult fabrication procedures.

Compared to gridded electrostatic thrusters of the 1960-70 period, the closed-drift thrusters had much lower efficiencies. For a proper historical perspective, it should be kept in mind that the 5000-10,000 s range of interest for specific impulse resulted from early projections of very light-weight power sources, and interest in interplanetary missions. As a result of these lower efficiencies, much of this early work on closed-drift thrusters ceased about 1970.

However, other programs involving closed-drift thrusters continued.<sup>10-34</sup> About the time that the space-charge-sheath type of thruster<sup>8</sup> was operated, an analysis of the closed-drift acceleration process showed that two distinctly different acceleration processes could take place.<sup>12</sup> In one case the electrons in the acceleration region were assumed to be at a negligible temperature (zero). The potential variation

---

Harold R. Kaufman is a Professor Emeritus of Colorado State University and is currently engaged in independent consulting and research. Prior to leaving Colorado State University, he was a Professor of both Physics and Mechanical Engineering. For the last six years he was also Chairman of the Physics Department. Before going to Colorado State University in 1974, he was employed for 23 years by NASA (and NACA) Lewis Research Center in Cleveland. Dr. Kaufman has a B.S. degree from Northwestern University and a Ph.D. from Colorado State University, both in Mechanical Engineering. His professional experience includes 7 years in airbreathing propulsion and 26 years in electric propulsion and plasma physics. He was the originator of the broad-beam electron-bombardment ion source, used in both space propulsion and ground industrial applications. Dr. Kaufman has authored more than 100 publications. He is an Associate Fellow of AIAA and has received both the AIAA Wyld Propulsion Award and the NASA Medal for Exceptional Scientific Achievement.

throughout the acceleration region then was found to be smooth and continuous, as had been implicitly assumed in the earlier closed-drift thruster work. If, however, the electrons were assumed to heat up as they flowed from the ion exhaust to the ion formation region, then a near-discontinuous potential jump occurred at the positive end of the acceleration channel. The remainder of the acceleration was assumed to take place in an axial length of the order of the local electron-cyclotron orbit.

With this acceleration model to serve as a guide, experimental verification of this anode-layer acceleration process was soon found in studies of the Penning discharge.<sup>35-40</sup> Subsequent studies of the Penning discharge gave additional verification and information.<sup>41-49</sup> These and other studies made clear some of the distinctions between the two types of closed-drift thruster.

In the first type of thruster, with a relatively long acceleration channel and dielectric wall (see Fig. 1), collisions of energetic electrons and ions with the dielectric walls served to emit low-energy secondary electrons. The high conductivity along magnetic field lines permitted energetic electrons to reach the walls and be replaced continuously by low-energy secondaries. This process served to limit the electron temperature to a moderate value in the acceleration region. As a result of the continuous and extended acceleration process, this type of thruster has been called a closed-drift extended-acceleration (CDEA) thruster in recent work.<sup>14-16,18,31,34</sup>

In the other type of thruster (see Fig. 2), the short channel walls give less opportunity for ion and electron collisions with the walls. Further, the metallic channel walls in this type of thruster are at the potential of the electron emitter, so that (except for the high-energy "tail" of a turbulent electron distribution) electrons will be reflected from the walls. The electrons, therefore, will tend to conserve total energy as they flow toward the anode, resulting in an increased electron temperature as the anode is approached. At some point, the increase in electron temperature will result in a downstream contribution to electron diffusion that will equal the upstream component due to the potential gradient. This point is the downstream boundary of the potential jump to near anode potential. This type of thruster is called, appropriately enough, an anode-layer thruster in recent work. It should be noted that this thruster type is very similar to the space-charge-sheath thruster studied earlier.<sup>8,9</sup>

Because the majority of both the total work and the recent work on closed-drift thrusters has used the CDEA and anode-layer designations, these designations will be used for the two major types in the remainder of this paper.

### Operating Characteristics

The typical single-stage closed-drift thruster requires one major power supply for the discharge between the electron-emitting cathode and the anode. If permanent magnets are not used, an auxiliary supply will be required for the magnet winding. A heating supply also will be required if a refractory-filament cathode is used. If a hollow cathode is used, a separate power supply will be required for initiation of the cathode discharge. Depending on the hollow-cathode design, no power supply may be required for its operation after it is started and coupled to the main discharge.

The operating characteristics of the main discharge are of particular interest. The characteristics of a single-stage CDEA thruster can be deduced from a large number of publications, but are described in a compact form by Morozov et al.<sup>14</sup> Information is less complete for the single-stage anode-layer thruster, but most of what is available appears to be similar to that of the CDEA thruster. The following general description therefore applies directly to a CDEA thruster, but should, for the most part, also apply to an anode-layer thruster. Where differences appear to exist for the two closed-drift thruster types, these differences will be pointed out.

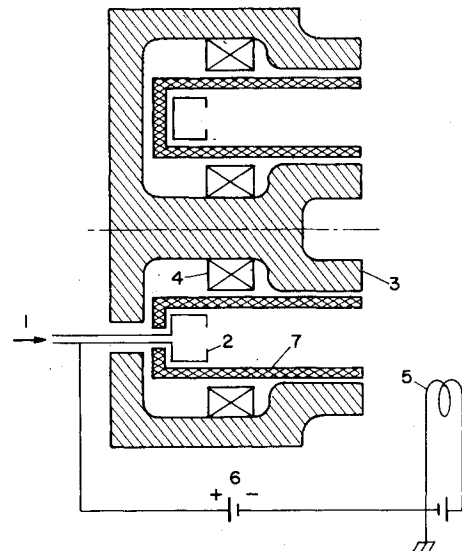


Fig. 1 Hall current or closed-drift extended-acceleration (CDEA), thruster (single stage). 1) Propellant feed; 2) anode distributor; 3) magnetic circuit, pole pieces; 4) magnet winding; 5) cathode neutralizer; 6) discharge power supply; 7) insulator.

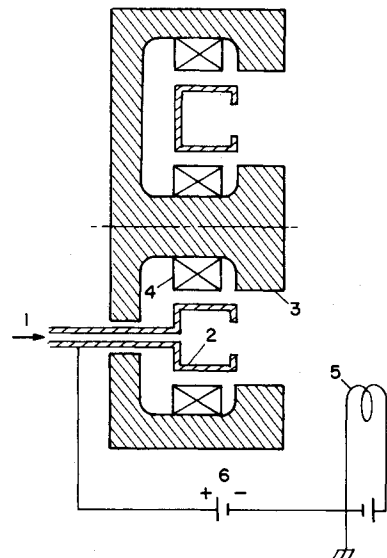


Fig. 2 Anode-layer thruster (single stage). 1) Propellant feed; 2) anode distributor; 3) magnetic circuit, pole pieces; 4) magnet winding; 5) cathode neutralizer; 6) discharge power supply.

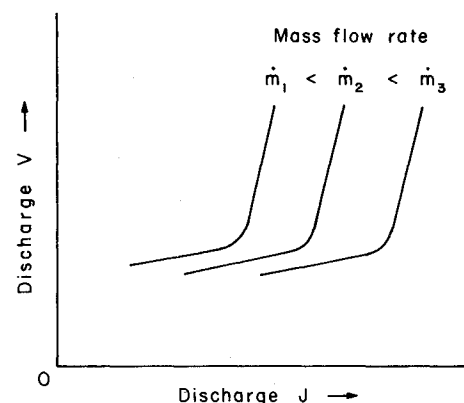


Fig. 3 Discharge characteristics for single-stage closed-drift thruster. (Magnetic field strength held constant.)

Assuming both the mass flow rate and the magnetic field strength are held constant, the current-voltage characteristics for the range of most interest can be approximated as a nearly constant-voltage region below a "knee" and a nearly constant-current region above (see Fig. 3). The current at the knee is roughly related to the current-equivalent of the mass flow rate, calculated with one electronic charge assigned per atom or molecule. To the extent that the propellant utilization is less than unity, the current at the knee will be reduced. The electron backflow to establish the accelerating electric field and double ionization will both tend to increase the knee value of current. The actual current value will include all of these effects, with some approximate overall relationship with the mass flow rate.

The sharpness of the discharge-characteristic knee is most evident with easily ionized materials, such as cesium and xenon. Figure 3 is characteristic of such an easily ionized material. With a less easily ionized material, such as argon, the curve shape can become much more rounded than is indicated in Fig. 3, so that a "knee" is only vaguely defined.

To a first approximation, the accelerated ion current will be a constant fraction of the discharge current in Fig. 3. The operation in the nearly constant-voltage region therefore corresponds to a range of propellant utilizations, with the highest utilization obtained at the highest current. The nearly constant-current region is also called the current saturation region.

Because charged particles with both signs are present in the acceleration region, there is no space-charge limit for the current density of the accelerated ions. Ion current densities in the  $A/cm^2$  range therefore are practical.<sup>6,13</sup>

Oscillations and fluctuations are generally observed in the operating regions of interest for a closed-drift thruster.<sup>16</sup> A typical disturbance in the nearly constant-voltage region is an ionization, or drift, wave. The fundamental mode of an ionization wave has a wavelength equal to the mean circumference of the annular channel. The wave velocity is lower than the electron drift velocity,  $E/B$ , typically by a factor of several. The frequencies observed for ionization waves are normally in the tens of kHz range, with a discrete frequency for the fundamental the usual dominant mode.<sup>16</sup> Because an ionization wave is driven by variations in the ion production rate, its amplitude decreases as the discharge current is increased and the utilization increased.

A typical disturbance in the nearly constant-current region is the transit-time oscillation.<sup>16</sup> This type of oscillation has a broad band of high frequencies. The center of this broad band roughly corresponds to the ion transit time through the acceleration channel. The amplitude of this oscillation increases with discharge voltage and can reach 20-30% of the mean applied voltage.

The amplitudes of these two types of oscillations tend to decrease as the knee is approached. Although there are varying degrees of overlap of the two oscillations near the knee, this region is one of comparative stability. This stability, together with high utilization, makes the general vicinity of the knee the preferred region for thruster operation. If the ion beam current is to be varied, the mass flow rate should also be varied so as to maintain the operation near the knee (see Fig. 3).

In the above discussion, two main types of oscillations have been emphasized. Other types of oscillations are also possible, including system oscillations, which depend on power-supply characteristics. Even with these other oscillations present, the knee region is still, in general, the preferred operating region.

The effect of varying the magnetic field strength is indicated in Fig. 4 for a fixed discharge current.<sup>14</sup> The mass flow rate is also assumed constant, at a value sufficient to avoid operation above the discharge-characteristic knee. The discharge voltage under these conditions (Fig. 4a) tends to increase with increasing magnetic field strength and then level off above some critical magnetic field. The fraction of the

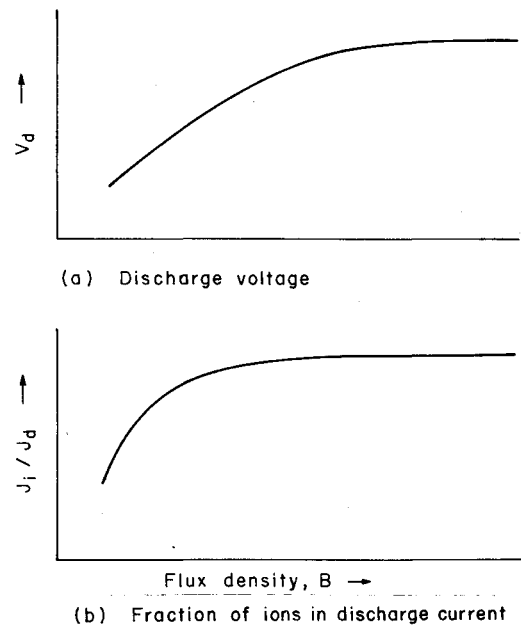


Fig. 4 Effect of magnetic field strength on operation of single-stage closed-drift thruster.

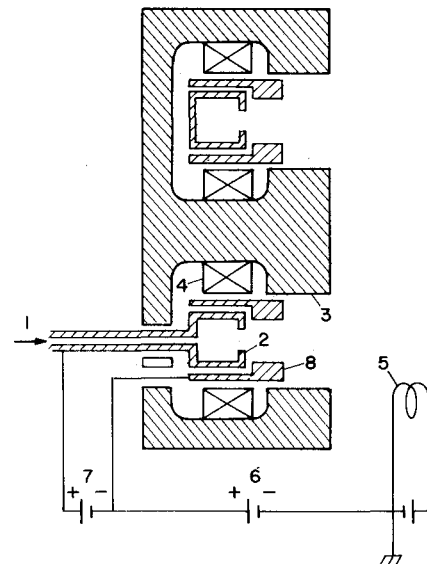


Fig. 5 Two-stage anode-layer thruster. 1) Propellant feed; 2) anode distributor; 3) magnetic circuit, pole pieces; 4) magnet winding; 5) cathode neutralizer; 6) acceleration-stage power supply; 7) ionization-stage power supply; 8) intermediate electrode.

current through the main power supply (termed discharge current herein) that results from accelerated ions (Fig. 4b) follows a similar trend. Useful values of the ion current typically range from 50-70% of the total discharge current.

The critical magnetic field is believed to be an artifact of the walls of the acceleration channel, inasmuch as bulk diffusion considerations alone would indicate a monotonic increase of voltage with an increasing magnetic field.

From the limited available<sup>14,28</sup> and physical considerations, it is believed that the relative trends of Fig. 4 differ for CDEA and anode-layer thrusters. As will be discussed in the next section, the temperature of the backstreaming electrons in a CDEA thruster tends to be limited by wall processes. The production of ions will thus tend to be related linearly to the backstreaming electron current in such a thruster. The matching condition for the ion production and acceleration portions of a CDEA thruster therefore will result in a nearly

constant-current ratio,  $J_i/J_d$ , over a broad range of operating conditions. For a CDEA thruster, then, the nearly constant region of  $J_i/J_d$  in Fig. 4b should extend over most of the range of voltage shown in Fig. 4a.

For an anode-layer thruster, though, the temperature of the backstreaming electrons, as they reach the ion production region, should vary nearly linearly with total applied voltage. A given ion current therefore should be produced with less backstreaming electron current at higher applied voltages. For moderate voltages, up to several hundred volts, the matching condition for ion production and acceleration would be expected to shift with voltage, giving a monotonically increasing value of  $J_i/J_d$  with increasing voltage.

Multistage closed-drift thrusters (see Fig. 5) have also been investigated. An additional cathode, at the potential of the intermediate electrode, has been optional.<sup>29-31</sup> The advantage of a multistage design is that the ion production process can be made more independent of the acceleration process. For example, a high-current, low-voltage stage can be used to form the ions. Then the electron backflow can be minimized through the high-voltage accelerating stage, thereby maximizing acceleration efficiency. It appears that any efficiency advantage for a multistage thruster should be greatest at high acceleration voltage. For low-voltage thrusters, particularly of the anode-layer type, the energy of the backstreaming electrons can be used effectively for ion production. The multistage approach therefore may be less efficient at low voltages.

There are also some specific details of closed-drift thruster designs that are important. Departures from circumferential uniformity by 5-15% for various parameters can cause large adverse effects on performance.<sup>27,29</sup> For neutral flow, though, the uniformity requirement refers to the general circumferential variation. The use of 20 uniformly spaced holes apparently had no adverse effect relative to a circumferentially uniform annular opening.<sup>20,21</sup>

The foregoing discussion also implicitly assumes passive pole-piece surfaces. If electron-emissive coatings are possible, a wide range of adverse effects can be obtained.<sup>27</sup> When using propellants such as cesium, it is preferable to have the thruster hot enough to avoid any significant condensation on internal surfaces.

Lifetime information is quite limited. Values of up to 1000 h are given for CDEA thrusters.<sup>33,34</sup> It is suspected that the ion bombardment of the insulating channel walls causes degradation of the insulator surface, eventually causing substantial surface conductivity. This process would be voltage and propellant dependent, so that more inert propellants and lower voltages would tend to give longer lifetimes. With this mode of failure, it is possible that large increases in lifetime, above the 500-1000 h range, may not be practical.

In the anode-layer thruster, only conducting surfaces are exposed to energetic ions. Greater lifetimes therefore should be possible with an anode-layer thruster than a CDEA thruster, with other operating aspects assumed to be similar. The electrode erosion in an anode-layer thruster appears to be caused primarily by off-axis trajectories of energetic ions near the edges of the ion beam.<sup>19,34</sup> The scaling law for this erosion process is not clear at present, but, using moderate extrapolation from CDEA tests, lifetimes of up to several thousands of hours should be readily possible. Required thrust durations for various missions tend to vary roughly with specific impulse, so that a few thousand hours may be adequate for many missions in the 1000-2000 s range of specific impulse.

### Electron Diffusion

It should be apparent that electron diffusion across a magnetic field is an important aspect of closed-drift thruster operation. As mentioned previously, an early and important

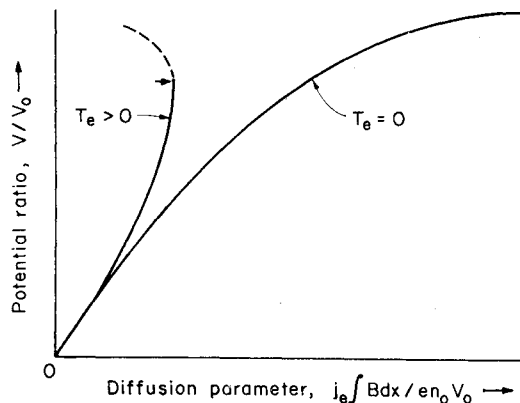


Fig. 6 Forms of solutions for  $1/B$  electron diffusion in closed-drift acceleration.

analysis of electron diffusion indicated the qualitative difference between CDEA and anode-layer acceleration.<sup>12</sup> This analysis was carried out assuming  $1/B^2$  classical diffusion, which was experimentally found to be orders of magnitude too low. The use of classical diffusion in this critical analysis apparently has led to some confusion as to whether classical diffusion is required for anode-layer thruster operation.<sup>14</sup>

The early diffusion analysis<sup>12</sup> has since been repeated with the assumption of  $1/B$  anomalous diffusion,<sup>50</sup> which is more consistent with experimental observations. The assumption of uniform and constant electron-current density (in the direction counter to ion acceleration), together with  $1/B$  diffusion results in the integral  $\int B dx$  being the significant magnetic parameter. This mathematical approach apparently was used first in the diffusion calculations for the discharge chamber of a gridded electrostatic thruster.<sup>51\*</sup>

The two general forms of analytical results obtained for the acceleration region of a closed-drift thruster are indicated in Fig. 6. The plasma potential is defined as zero at the accelerator exhaust plane and  $V_0$  at the source potential for the ions. The potential parameter  $V/V_0$  thus increases from zero to unity when moving from the accelerator exhaust to the source of the ions. In the electron diffusion parameter,  $j_e$  is the axial electron-current density (assumed to be a constant),  $B$  the transverse flux density,  $x$  the axial distance measured from the exhaust plane,  $e$  the electronic charge, and  $n_0$  the electron (or ion) density at the exhaust plane. For a given thruster configuration and operating condition, only the integral  $\int B dx$  is a variable, which increases from zero to a maximum when going from the exhaust plane to the upstream end of the closed-drift acceleration region.

In one form of solution, the potential ratio  $V/V_0$  increases smoothly and continuously from 0 to 1 when passing through the acceleration region. This solution is obtained only for a zero electron temperature throughout the acceleration region. The other form of solution is obtained when the electron temperature is greater than zero. In this form the electron diffusion downstream due to a finite electron temperature at some point becomes equal to the upstream diffusion due to the potential gradient. At this point, indicated by an arrow in Fig. 6, the slope of the potential variation becomes infinite. The mathematical solutions can be continued beyond this

\*The integral  $\int B dx$  (or  $\int \mathbf{B} \times d\mathbf{x}$ ) has significance from several viewpoints. It is the proper magnetic parameter for the deflection of an isolated charged particle passing through a region of uniform potential, but varying magnetic field strengths.<sup>52</sup> It was later shown to be the proper parameter for a charged particle passing through a region in which both the plasma potential and the magnetic field strength varied.<sup>53</sup> It is also an empirical parameter for closed-drift acceleration, based on the observation that the local time-averaged electric field varied approximately as the local magnetic field strength.<sup>14</sup>

point, as shown by the dashed line, but they become physically meaningless.

In terms of physical application, the two types of solutions indicated in Fig. 6 can be organized into two other categories. In the first category, the electron temperature is assumed constant throughout the acceleration region. This category also includes the unique zero-temperature solution of Fig. 6. The diffusion-parameter values for the entire closed-drift acceleration region are then given by<sup>50</sup>

$$\frac{j_e \int B dx}{en_0 V_0} = \frac{1}{8} \left[ 1 + \frac{T}{2V_0} - \left( 1 - \frac{V}{V_0} \right)^{1/2} - \frac{T/V_0}{2(1 - V/V_0)^{1/2}} \right] \quad (1)$$

The corresponding maximum values for  $V/V_0$  are given by

$$V/V_0 = 1 - T/2V_0 \quad (2)$$

Note that the value of  $V/V_0$  goes to unity as  $T/V_0$  goes to zero. The general form of the solutions indicated by Eqs. (1) and (2) depends on  $1/B$  electron diffusion. The numerical constants result from the assumption of the Bohm value for this  $1/B$  diffusion.

Because the maximum value of  $V/V_0$  is  $<1$  for  $T/V_0 > 0$ , there will, in general, be an infinite slope of potential at the upstream end of the acceleration region. If the ions are assumed to come from a plasma located at the upstream end of the acceleration region, it is reasonable to assume that they are accelerated to ion acoustic velocity before leaving the ion production region (the Bohm condition for a stable sheath). If the background electrons in the production and acceleration regions are at the same temperature, the acceleration will be just sufficient to reduce the plasma potential at the boundary of the ion production region to the value given by Eq. (2).

For ion production in a plasma, then, constant electron temperature in the acceleration region implies the absence of a potential discontinuity between the production and acceleration regions. Note that this conclusion is dependent on the production of ions in a plasma. If contact ionization is used, for example, a potential jump of  $T/2$  will be found close to the ionizer.

In the second category of solutions the electron energy is assumed to be conserved as the electrons flow upstream. This results in a temperature rise, in eV, equal to two-thirds the potential difference, in V, through which the electron passes. The diffusion parameter values for the entire closed-drift acceleration region are then given by<sup>50</sup>

$$\frac{j_e \int B dx}{en_0 V_0} = \frac{1}{24} \left[ 5 + \frac{3T_0}{2V_0} - 4 \left( 1 - \frac{V}{V_0} \right)^{1/2} - \frac{2 + 3T_0/V_0}{2(1 - V/V_0)^{1/2}} \right] \quad (3)$$

The corresponding maximum values for  $V/V_0$  are given by

$$V/V_0 = \frac{3}{4} (1 - T_0/2V_0) \quad (4)$$

Because the electron temperature varies throughout the acceleration region,  $T_0$  is the electron temperature in the exhaust plane.

For the production of ions in a plasma,  $T_0$  should also approximate the temperature of background electrons in this plasma. The normal acceleration of ions by a potential difference of  $T_0/2$  will not be sufficient to avoid a potential discontinuity at the junction of the production and acceleration regions. This discontinuity, which exists from the viewpoint of continuum equations, should be accommodated by a single, collision-free electron orbit.<sup>50</sup>

Experimentally, the constant electron-temperature solutions should be approximated with CDEA thrusters, where collisions of ions and energetic electrons with the insulating walls will result in the continual replacement of

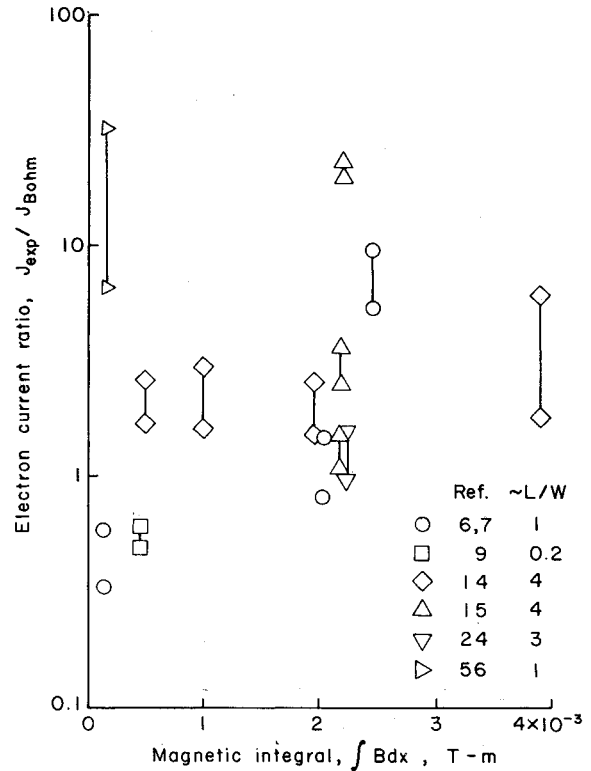


Fig. 7 Ratio of experimental-to-theoretical electron currents, with Bohm diffusion used for the theoretical value. Two symbols connected by a line represent a range of operation or a group of data points.

energetic electrons by lower energy secondary electrons.<sup>32</sup> In the anode-layer type, this exchange process is generally prevented and the acceleration process should approximate the conserved energy solutions.

Experimental electron backflows were compared with the theoretical predictions of Eqs. (1-4) for several closed-drift thrusters, as presented in Fig. 7. All of these data were analyzed with the constant-temperature solutions of Eqs. (1) and (2), except for the data of Ref. 9. These last data were obtained with a channel length-to-width ratio of  $\sim 0.2$ . Even though an insulating coating was used on the channel walls, there was little opportunity for many wall collisions in such a short channel, and the conserved-energy solutions of Eqs. (3) and (4) were used instead. The data were generally incomplete, so that assumptions were necessary for such parameters as electron initial, or constant, temperature. These assumptions were felt to contribute an uncertainty in the final values of Fig. 7 of less than  $\pm 20\%$ .

The experimental-to-Bohm electron current ratios in Fig. 7 range over two decades, with no readily apparent dependence on the magnitude of the magnetic integral. The data presented in Fig. 7 include a wide range of designs, some of which are known to be poor. Eliminating the data from poor designs therefore should result in a reduction of the range of electron current ratio.

The data of Morozov et al.<sup>15</sup> included a magnetic field configuration that was strongest at the upstream end of the channel, another that was uniform, and still another that was strongest at the downstream end of the channel. The highest ratios of  $J_{\text{exp}}/J_{\text{Bohm}}$  were for the former, while the lowest were for the latter (see the three groups of data in Fig. 7). One way of interpreting these results is to recognize that the channel length-to-width ratio (axial channel length divided by the difference of the inside and outside channel radii) was about 4 for these data, and it has been observed that only the downstream portion of a long channel is effective.<sup>26</sup> The

efficiency of a long acceleration channel thus is improved by concentrating more of the total magnetic field near the exhaust plane, in effect making the channel shorter. Another interpretation, perhaps equivalent, is that ions produced in the upstream portion of a long channel have little chance of escape without striking the channel walls. Concentration of the magnetic field at the upstream end of the channel therefore should be expected to concentrate ion production further upstream, thereby decreasing the electrical efficiency. Only the data for lowest group in Fig. 7, for which the magnetic field was concentrated at the downstream end, are included from this reference in Fig. 8. The data from Plank et al.<sup>56</sup> also were excluded from Fig. 8 due to known large circumferential variations in the magnetic field.

The remaining data were replotted against the normalized magnetic field integral in Fig. 8. The normalized integral is defined as the experimental integral at the mean radius, divided by the integral required to barely prevent an initially stationary electron from directly (without a collision) reaching the anode. This minimum integral required to prevent a direct trajectory is  $(2m_e V/e)^{1/2}$ . For the normalized integral range from about 3 to 50, the experimental electron current is within about a factor of 3 of the value predicted using Bohm diffusion. At higher values of normalized integral, the experimental current from two investigations rises higher, up to about 10 times the Bohm value, even though there is no apparent flaw in the thruster designs used.

The increase of anomalous electron diffusion above the classical value is most often attributed to potential fluctuations within the bulk of the plasma.<sup>†</sup> Morozov et al.<sup>14</sup> have pointed out that wall effects could also cause anomalous diffusion. The rough agreement with Bohm diffusion over a large range of normalized magnetic field integrals suggests a single anomalous-diffusion mechanism. The rise in experimental currents at high values of normalized integral suggests a second mechanism. It is common in a wide range of experimental investigations to observe a shift from one mode of operation to another as an operating parameter is indefinitely increased. It would not be surprising if anomalous diffusion in closed-drift thrusters shifted from being caused by bulk fluctuations to being caused by wall effects, or vice versa, as the magnetic field is increased.

Summarizing the conclusions drawn from Fig. 8, the electron diffusion in closed-drift thrusters appears to be within about a factor of 3 of Bohm diffusion for a wide range of normalized magnetic field integrals, but rises sharply at the highest normalized integrals. Detailed considerations of ion losses at channel walls suggest that the agreement with Bohm diffusion would be improved further by restricting channel length-to-width ratios to  $\leq 1$ . The drop in the maximum values of  $J_{\text{exp}}/J_{\text{Bohm}}$  might be as much as 30-40% for such a channel length restriction in the 3-50 range for the normalized integral. Although operation at normalized integrals higher than 50 is possible, the data of Fig. 8 indicate that the electron backflow will simply increase continuously above the Bohm value for these higher integrals.

It should be noted that the approximate limit of 50 for the normalized magnetic integral is not understood from a theoretical viewpoint. New designs or operating regimes therefore might drastically alter this limit. However, if a normalized integral of 50 is used, together with Bohm diffusion, the minimum ratio of electron backflow to xenon ion acceleration,  $J_e/J_i$ , is about 0.5. This value is in reasonable agreement with experimental values for this minimum ratio. Diffusion theory also indicates that this minimum ratio should vary as the square root of propellant atomic mass, but the limited data do not support this conclusion.<sup>6,9,14,15,28</sup>

<sup>†</sup>A recent analytical study of diffusion indicates that roughly the Bohm level of diffusion would be expected from thermal fluctuations alone.<sup>57</sup>

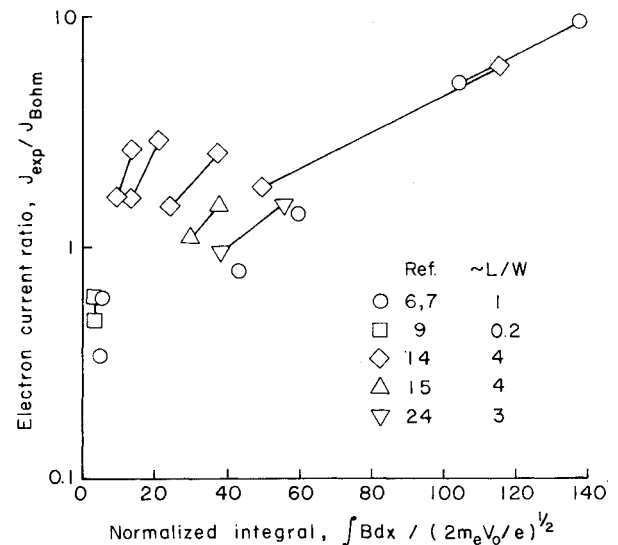


Fig. 8 Ratio of experimental-to-theoretical electron currents as a function of the normalized magnetic integral.

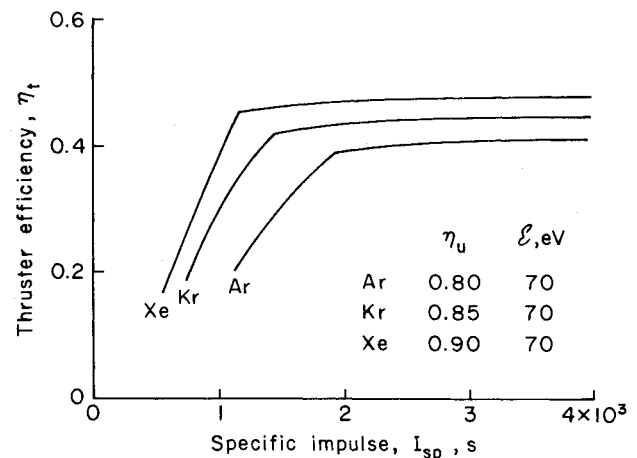


Fig. 9 Theoretical performance for single-stage closed-drift thruster with inert-gas propellants.

Instead, a constant minimum ratio of about 0.5 appears to be a reasonable value of all propellants. Because of the limited data, however, this conclusion can be considered only tentative.

### Ion Production

The other important aspect of closed drift thruster operation, besides electron diffusion in the acceleration region, is the production of ions. The losses in this production process consist of both the electron energy required for ion production and the escape of neutrals.

The anode-layer thruster should have an inherent advantage over the CDEA thruster in terms of efficiency, by using energy from backstreaming electrons to generate ions more effectively. For that reason, the anode-layer thruster is emphasized in the discussion of this section. Because of the basic similarity of all closed-drift thrusters, the conclusions reached will also have considerable validity for CDEA thrusters.

Most of the ion generation in an anode-layer thruster occurs in a thin layer at the upstream end of the acceleration region.<sup>29</sup> This layer has a thickness of the order of the dimensions of the electron-cyclotron orbit. The ion production process in this thin layer can be approximated from existing knowledge of gridded thruster operation.

Considering first the discharge energy required for ion production, a recent gridded thruster investigation using argon indicated 70-80 eV/ion on a total volume production basis.<sup>58</sup> There have been many such studies in the past, but this recent study was selected because of the new developments in this field. On the basis of limited data, the general assumption was made previously that ions generated in the discharge chamber of a gridded thruster flow nearly equally to all discharge-chamber boundaries. This assumption was satisfying, in that it was also consistent with ion flow at ion acoustic velocity in all directions from the region of production.

It was experimentally determined in this recent study, however, that the ions were directed preferentially away from any boundary in which a transverse magnetic field existed, and an outward flow of electrons took place across this magnetic field.<sup>58</sup> Theoretical considerations were also used to show that the directed ion flow toward such a boundary had to take place at far below ion acoustic velocity. To the first approximation, therefore, all ions should be expected to be directed away from a boundary with both a transverse field and an outward flow of electrons.

These conditions are, of course, precisely the conditions in the ion production region of an anode-layer thruster. With a thin ion production region and typical ion beam dimension, essentially all ions should be directed away from the anode and therefore into the ion beam. From knowledge of ion production in gridded thrusters, then, the discharge loss for "knee" operation should be 70-80 eV/ion. From previous experience with various inert gases, this discharge loss should be roughly the same for argon, krypton, and xenon.

This discharge-loss value is supported by a detailed study of ion production and energy losses in a CDEA thruster operated on xenon.<sup>26</sup> Based on the ion beam extracted, a production loss of roughly 100 eV/ion was obtained. Correcting for the wall losses, which should be greatly reduced in an anode-layer thruster, the production loss for total ion production was found to be 60-70 eV/ion.

A discharge loss on the order of 70 eV/ion therefore appears reasonable for an anode-layer thruster operating on inert gases from argon through xenon. Depending mostly on the length of the acceleration channel, the losses for a CDEA thruster would be expected to be higher. Some variation of discharge loss would be expected with propellants having significantly different ionization potentials. But experience indicates that the discharge loss variation is considerably less than linear with ionization potential.<sup>59</sup>

The other major loss that should be considered is the escape of neutral, or nonionized, propellant. The operation of a low-pressure discharge to generate ions has been found to depend on the maintenance of a minimum neutral density, with the exact value of neutral density dependent on the geometry of

the ion production region.<sup>59</sup> For an anode-layer thruster, the pertinent geometry parameter is the depth of the ion production region. This depth, as mentioned earlier, is of the order of an electron-cyclotron orbit. From existing theory, then, the loss rate of neutrals, expressed as an equivalent current density, is expected to vary as

$$j_0 = K_I B / V_0^{1/2} \quad (5)$$

where  $K_I$  is some constant that depends on the propellant,  $B$  the magnetic-field strength in the ion production region, and  $V_0$  the discharge voltage. Numerical evaluation of the constant  $K_I$  indicates a value on the order of  $10^5$  for xenon. For a typical operating condition of  $2 \times 10^{-2}$  T and 200 V, the equivalent current density of the neutral loss should be roughly 0.1-0.2 A/cm<sup>2</sup>. It should be evident from this neutral loss that an anode-layer thruster must operate in the A/cm<sup>2</sup> range for the extracted ion beam if an acceptable propellant utilization is to be obtained. A CDEA thruster would be expected to have slightly lower neutral losses due to the extended ionization zone, but not substantially lower.

The experimental measurements of propellant utilization in closed-drift thrusters are limited,<sup>14,28</sup> but consistent with the general picture presented above. Experimentally, a magnetic field configuration which increases in strength in the downstream direction has been found desirable. From Eq. (5), such a variation permits the ion production region to be in a low magnetic field strength region, thereby reducing neutral losses. At the same time, the high field strength in the acceleration region generally is desirable to reduce electron diffusion in the upstream direction. This type of magnetic field variation thus tends to accommodate the conflicting requirements of ion production and acceleration.

If high ion-beam current densities are required to obtain high propellant utilizations, the upper limit on the permissible ion-beam current density is of interest. One limit, of course, is a need to radiate, or otherwise reject, waste energy. From available literature, this has not appeared to be a serious limitation. Another limit can be that of required lifetime, with excessive current densities resulting in unacceptably short lifetimes. Duration tests clearly are required to determine this limit.

Still another limit is that of the ratio of acceleration force relative to the magnetic field force. That is, if the current density of accelerated ions is sufficiently large, the reaction of this acceleration force will seriously distort the magnetic field. It would be expected that the maximum ion-beam current density from this consideration is of the form

$$j_i = K_2 B^2 / V_0^{1/2} \quad (6)$$

with the value of  $K_2$  dependent on the exact configuration used. If the acceleration force per unit beam area is simply set equal to the stress in the magnetic field,  $B^2/2\mu_0$ , the value of the constant  $K_2$  for xenon is about  $2.4 \times 10^8$ . For the previously used conditions of  $2 \times 10^{-2}$  T and 200 V, the maximum current density is found to be about 0.7 A/cm<sup>2</sup>. This limitation will, as mentioned, depend on the exact configuration used. It should be clear, however, that it can be a very real limitation to maximizing propellant utilization.

### Scaling

The previous sections have emphasized details of design and operation. General overall performance trends with major dimensional changes are also of interest. The two major dimensions of a closed-drift thruster are the magnetic integral  $\int B dx$  and some characteristic length  $L$ .

The magnetic integral determines the electron backflow through the acceleration region. From Eqs. (1) and (3), this

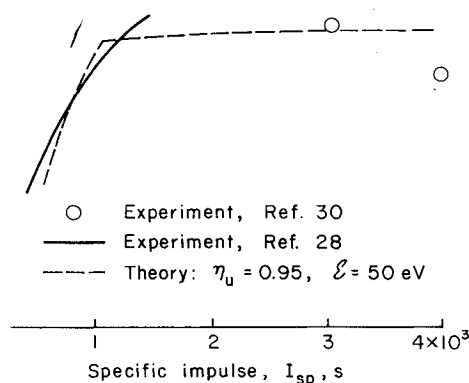


Fig. 10 Comparison of theory and experiment for cesium propellant. (A single-stage anode-layer thruster was used in Ref. 28, and a two-stage anode-layer thruster was used in Ref. 30.)

electron backflow is of the form

$$j_e \{Bdx\} / en_0 V_0 = K_3 \quad (7)$$

where  $K_3$  depends on the electron temperature variation through the acceleration channel. Inasmuch as the ion current density  $j_i$  is proportional to  $en_0 V_0^{1/2}$ , Eq. (7) can be rewritten as

$$j_e/j_i = K_3' V_0^{1/2} / \{Bdx\} \quad (8)$$

or

$$j_e/j_i = K_3'' / (\{Bdx\})_{\text{norm}} \quad (9)$$

where  $(\{Bdx\})_{\text{norm}}$  is the normalized magnetic integral, as used in Fig. 8.

At low applied voltages (and low exhaust velocities), the ratio of  $j_e/j_i$  is determined by the electron backflow required to ionize the propellant. As the voltage is increased, the required electron current decreases. From Eq. (8), for  $j_e/j_i$  to decrease as  $V_0$  is increased,  $\{Bdx\}$  must increase more rapidly than  $V_0^{1/2}$ . This decrease in  $j_e/j_i$  continues until  $j_e/j_i$  reaches a minimum, which is associated with a maximum value of the normalized magnetic integral (herein assumed to be about 50). For all higher voltages,  $\{Bdx\}$  should increase with  $V_0^{1/2}$ .

The selection of the proper magnetic integral thus depends primarily on the desired operating voltage. As described in connection with Fig. 3, hard-to-ionize propellants have poorly defined regions of optimum operation. The relation of magnetic integral with applied voltage will be less clearcut with such propellants. On the other hand, propellants with low ionization potentials and large cross sections will tend to have a closer relation between the magnetic integral and  $V_0$ .

If the operating voltage is assumed to be fixed, the effect of size can be determined by varying the characteristic dimension  $L$ . For simplicity, all other spatial dimensions were assumed to vary with  $L$ . Because the voltage is fixed, the magnetic integral should also be fixed. If  $\{Bdx\}$  is to be fixed while  $L$  varies, then  $B$  should vary inversely with  $L$ .

$$B \sim 1/L \quad (10)$$

From considerations of magnetic field stress, Eq. (6) gives a maximum ion current density of the form

$$j_i \sim B^2 \quad (11)$$

Combining relations (10) and (11).

$$j_i \sim 1/L^2 \quad (12)$$

The total ion current,  $J_i$ , is the product of beam area and ion current density. Because beam area varies as  $L^2$ , the maximum ion current (from magnetic stress considerations) is independent of thruster size.

Note that this result depends, at higher voltages, on the existence of a maximum permissible normalized integral. If higher integrals can be used effectively, the limit on maximum ion current can be increased. At lower voltages, though, where the electron backflow is required for ionization, the maximum permissible ion current appears to be fundamentally independent of thruster size.

If thruster size can vary widely for the same ion-beam current, some basis other than ion-beam current should be used to select thruster size. For a more compact design, and probably also a lower thruster mass, a smaller size is preferred. It can also be shown that propellant utilization will tend to increase as thruster size is decreased.

From Eq. (5), the equivalent current density of the escaping neutrals varies as

$$j_0 \sim B \quad (13)$$

To maximize propellant utilization,  $j_i/j_0$  should be maximized. From relations (10), (11), and (13),

$$j_i/j_0 \sim 1/L \quad (14)$$

That is, propellant utilization is maximized by using the smallest possible thruster size.

There are other considerations in selecting thruster size. A thruster should be large enough to reject the waste energy (probably by radiation). It also appears likely that larger thrusters would tend to have longer lifetimes. As a general conclusion, then, the smallest possible thruster size should be used, consistent with heat rejection and lifetime requirements.

### Thruster Performance

In evaluating the suitability of closed-drift thrusters for particular missions, knowledge of their performance is essential. A procedure for predicting performance is presented in this section, together with available experimental data.

The general configuration assumed for calculation is a short, single-stage, closed-drift thruster with only one major power circuit. The magnetic field is assumed to be supplied either by a field winding with negligible power requirements, or by permanent magnets. The electron emitting cathode is assumed to be a hollow cathode, properly sized so that external power is not required for cathode heating or otherwise sustaining the discharge after it is started.

Having assumed a hollow cathode, a cathode-to-plume potential drop is also assumed with a value equal to the first ionization potential of the gas used. It is true that the ionization process is more complicated than simply injecting electrons at this potential, but experimental potential differences for hollow cathodes approximate this value. The required electron emission from the cathode will equal the electron backflow through the accelerating region plus the neutralizing current for the accelerated ions.

The electron backflow will be set by the maximum of two conditions. One is the minimum electron current required to produce the ions by a discharge process. The other is the minimum electron-to-ion current ratio.

From an earlier discussion, a discharge loss of 70 eV/ion was assumed for argon, krypton, and xenon. For cesium and cadmium, which have lower ionization potentials, 50 eV/ion was assumed. At low applied voltages, the electron backflow is set by this discharge-loss requirement.

As indicated earlier, when the applied voltage is increased, a constant discharge loss per ion results in a decreased requirement for electron backflow. Eventually, a minimum electron-to-ion current ratio is reached. Present experimental evidence indicates a minimum value for  $J_e/J_i$  of about 0.5.<sup>6,9,14,15,28</sup>

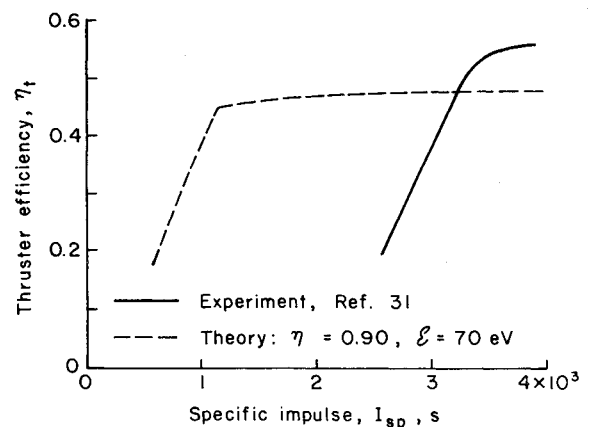


Fig. 11 Comparison of theory and experiment for xenon propellant. (A two-stage anode-layer thruster was used in Ref. 31.)



To summarize the procedure for inert gases, the electron emission process was assumed to result in a potential-difference loss equal to the first ionization potential. The electron backflow to the anode was then taken to be the largest of two values. One was the electron backflow required to produce ions at 70 eV/ion. The other was a minimum electron backflow equivalent to half the ion current. Using this procedure, together with a thrust coefficient of 0.90, power efficiencies were calculated. The assumed utilization efficiencies of 0.80, 0.85, and 0.90 are believed to be consistent with the limited experimental closed-drift thruster data,<sup>14,28</sup> and were used to convert power efficiencies into thruster efficiencies. These thruster efficiencies are plotted against specific impulse in Fig. 9. The break in each efficiency curve corresponds to the minimum specific impulse at which  $J_e/J_i$  reaches 0.5.

As shown in Fig. 9, the efficiency is highest with xenon. The difference between different propellants is small above about 2000 s. But in the 1000-2000 s range of specific impulse, which is believed to be particularly suited to closed-drift thrusters, the effect of propellant atomic weight is important.

Limited experimental data are available for comparison with this theoretical approach. The most complete data appear to be for cesium propellant.<sup>28,30</sup> These data are presented in Fig. 10, together with a theoretical prediction. This theoretical prediction was similar to that carried out for Fig. 9, except that the discharge loss was dropped to 50 eV/ion and the propellant utilization was increased to 0.95. These changes are believed to be consistent with the extremely low ionization potential and large ionization cross section of cesium, as well as the limited experimental closed-drift thruster data.<sup>28</sup>

The calculated performance is in excellent agreement with all experimental performance, except the data point near 4000 s. To provide the necessary exhaust velocity, the 4000 s point is at roughly 1000 V. With this high a discharge voltage, there would be a large fraction of the propellant that would be multiply ionized, resulting in increased thruster losses. Alternatively, the 4000 s point may not have been optimized experimentally. In the 1000-2000 s range of most interest, though, the calculation procedure appears to represent the experimental values with sufficient accuracy for a rough estimate of performance.

Limited data are also available for xenon propellant, and are shown in Fig. 11, together with the calculated xenon curve from Fig. 9. The thruster used in this case was a two-stage anode-layer type. It appears that this thruster was not designed to operate efficiently at low specific impulse. The maximum efficiency in the 3500-4000 s range, though, is in reasonable agreement with the calculated performance.

A final comparison can be made for cadmium propellant in a CDEA thruster. In this case, a fairly deep ( $L/W \approx 3$ )

channel is believed to be the cause of the experimental performance being significantly lower than the calculated performance (see Fig. 12).

### Concluding Remarks

The technology of closed-drift thrusters is reviewed. This type of thruster appears to have inherent advantages over both electrothermal and gridded-electrostatic thrusters in the 1000-2000 s range of specific impulse.

Electron diffusion across a magnetic field is a crucial aspect of closed-drift thruster operation. Experimental electron-diffusion data have been reviewed and compared with diffusion theory. A normalized magnetic field integral has been defined as the experimental integral  $\int B dx$  divided by the minimum integral that will prevent an initially motionless electron from reaching the anode at the discharge voltage used. Experimental electron diffusion was found to be within a factor of about 3 of the Bohm diffusion value over a range of normalized magnetic field integral from about 3 to 50. Above about 50, the experimental diffusion rose sharply, relative to the Bohm diffusion value. The sharp rise in electron diffusion was found to be related to the minimum electron-to-ion current ratio in the acceleration process.

The ion-production process was also analyzed. Because of the shallow depth of the ion production region, a closed-drift thruster (particularly of the anode-layer type) is essentially a high current-density device. To obtain useful propellant utilizations, the ion current densities should be in the A/cm<sup>2</sup> range. On the other hand, the discharge losses appear to be as low, or lower, than any competitive ion-beam sources.

A calculation procedure was presented for estimating the performance of a closed-drift thruster. Limited experimental data indicated that this procedure is adequate for rough performance estimates of single-stage thrusters with short acceleration channels.

The experimental and calculated performance indicate thruster efficiencies of about 0.5 are practical in the 1000-2000 s range of specific impulse, when using high ( $\geq 100$ ) atomic mass propellants.

### References

- <sup>1</sup>Seikel, G. R. and Reshotko, E., "Hall Current Ion Accelerator," *Bulletin of the American Physical Society*, Ser. II, Vol. 7, June 1962, p. 414.
- <sup>2</sup>Lary, E. C., Meyerand, R. C. Jr., and Salz, F., "Ion Acceleration in a Gyro-Dominated Neutral Plasma—Theory," *Bulletin of the American Physical Society*, Ser. II, Vol. 7, July 1962, p. 441.
- <sup>3</sup>Salz, F., Meyerand, R. C. Jr., and Lary, E. C., "Ion Acceleration in a Gyro-Dominated Neutral Plasma—Experiment," *Bulletin of the American Physical Society*, Ser. II, Vol. 7, July 1962, p. 441.
- <sup>4</sup>Seikel, G. R., "Generation of Thrust—Electromagnetic Thrusters," *Proceedings of the NASA-University Conference on the Science and Technology of Space Exploration*, Vol. 2, Nov. 1962, pp. 171-176.
- <sup>5</sup>Ellis, M. C. Jr., "Survey of Plasma Acceleration Research," *Proceedings of the NASA-University Conference on the Science and Technology of Space Exploration*, Vol. 2, Nov. 1962, pp. 171-176.
- <sup>6</sup>Pinsley, E. A., Brown, C. O., and Banas, C. M., "Hall-Current Accelerator Utilizing Surface Contact Ionization," *Journal of Spacecraft and Rockets*, Vol. 1, Sept./Oct. 1964, pp. 525-531.
- <sup>7</sup>Brown, C. O. and Pinsley, E. A., "Further Experimental Investigations of a Cesium Hall-Current Accelerator," *AIAA Journal*, Vol. 3, May 1965, pp. 853-859.
- <sup>8</sup>Meyer, R. X., "A Space-Charge-Sheath Electric Thruster," *AIAA Journal*, Vol. 5, Nov. 1967, pp. 2057-2059.
- <sup>9</sup>Meyer, R. X., "Laboratory Testing of the Space-Charge-Sheath Electric Thruster Concept," *Journal of Spacecraft and Rockets*, Vol. 7, March 1970, pp. 251-255.
- <sup>10</sup>Zeyfang, E., "Investigations on Ion Sources for Hall Ion Accelerators," *First International Conference on Ion Sources*, Saclay, June 1969.
- <sup>11</sup>Zeyfang, E., "A Plasma Source with Annular Slit Hollow Cathode for Hall Ion Thrusters," *III European Electric Propulsion Conference*, Oct. 1974.

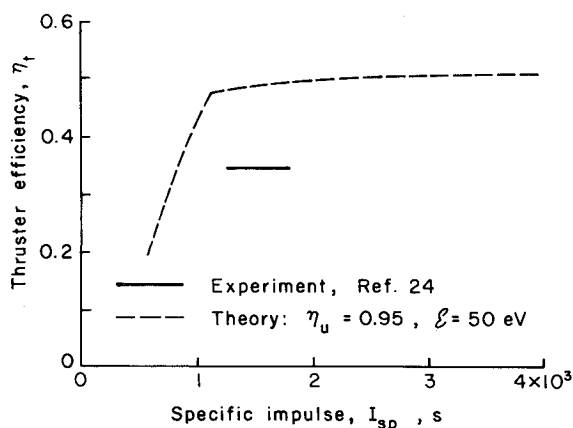


Fig. 12 Comparison of theory and experiment for cadmium propellant. (A single-stage CDEA thruster with a relatively deep ( $L/W \approx 3$ ) channel was used in Ref. 24.)

- <sup>12</sup>Zharinov, A. V. and Popov, Yu. S., "Acceleration of Plasma by a Closed Hall Current," *Soviet Physics-Technical Physics*, Vol. 12, Aug. 1967, pp. 208-211.
- <sup>13</sup>Zubkov, I. P., Kislov, A. Ya., and Morozov, A. I., "Experimental Study of a Two-Lens Accelerator," *Soviet Physics-Technical Physics*, Vol. 15, May 1971, pp. 1796-1800.
- <sup>14</sup>Morozov, A. I., Esipchuk, Yu. V., Tilinin, G. N., Trofimov, A. V., Sharov, Yu. A., and Shchepkin, G. Ya., "Plasma Accelerator with Closed Electron Drift and Extended Acceleration Zone," *Soviet Physics-Technical Physics*, Vol. 17, July 1972, pp. 38-45.
- <sup>15</sup>Morozov, A. I., Esipchuk, Yu. V., Kapulkin, A. M., Nerovskii, V. A., and Smirnov, V. A., "Effect of the Magnetic Field on a Closed-Drift Accelerator," *Soviet Physics-Technical Physics*, Vol. 17, Sept. 1972, pp. 482-487.
- <sup>16</sup>Esipchuk, Yu. V., Morozov, A. I., Tilinin, G. N., and Trofimov, A. V., "Plasma Oscillations in Closed-Drift Accelerators with an Extended Acceleration Zone," *Soviet Physics-Technical Physics*, Vol. 18, Jan. 1974, pp. 928-932.
- <sup>17</sup>Kervalishvili, N. A. and Kortkhondzhiya, V. P., "Low-Pressure Discharge in a Transverse Magnetic Field," *Soviet Physics-Technical Physics*, Vol. 18, March 1974, pp. 1203-1205.
- <sup>18</sup>Melikov, I. V., "Experimental Investigation of Anode Processes in a Closed Electron-Drift Accelerator," *Soviet Physics-Technical Physics*, Vol. 19, July 1974, pp. 35-37.
- <sup>19</sup>Yerofeyev, V. S. and Leskov, L. V., "Hall-Accelerator of Plasma with Anode Layer" (in Russian), *Physical Principles of Plasma Accelerators*, edited by A. I. Morozov, Nauka, Minsk, 1974, pp. 18-47.
- <sup>20</sup>Dem'yanenko, V. N., Zubkov, I. P., and Morozov, A. I., "Open Single-Lens Hall-Current Accelerator," *Soviet Physics-Technical Physics*, Vol. 21, Aug. 1976, pp. 987-988.
- <sup>21</sup>Melikov, I. V., "Point and Jet Ionization in a Hall Plasma Accelerator," *Soviet Physics-Technical Physics*, Vol. 22, April 1977, pp. 452-453.
- <sup>22</sup>Askhabov, S. N., Melikov, I. V., and Fishgoit, V. V., "Electric Discharge in Direct-Flow Hall Accelerator," *Soviet Physics-Technical Physics*, Vol. 22, April 1977, pp. 453-458.
- <sup>23</sup>Tilinin, G. N., "High-Frequency Waves in a Hall Accelerator with an Extended Acceleration Zone," *Soviet Physics-Technical Physics*, Vol. 22, Aug. 1977, pp. 975-978.
- <sup>24</sup>Trofimov, A. V., "Hall Accelerator with Cadmium Vapor," *Soviet Physics-Technical Physics*, Vol. 22, Oct. 1977, pp. 1280-1282.
- <sup>25</sup>Tilinin, G. N., "Modulation of the Ion Stream at the Exit from a Hall Plasma Accelerator with an Extended Acceleration Zone," *Soviet Physics-Technical Physics*, Vol. 22, Nov. 1977, pp. 1422-1423.
- <sup>26</sup>Bishaev, A. M. and Kim, V., "Local Plasma Properties in a Hall-Current Accelerator with an Extended Acceleration Zone," *Soviet Physics-Technical Physics*, Vol. 23, Sept. 1978, pp. 1055-1057.
- <sup>27</sup>Ivashchenko, S. S., Parshchik, A. S., Tkachenko, V. A., and Shipilov, Yu. V., "Operational Characteristics of an Anode-Layer Accelerator in Low-Voltage Modes" (in Russian), *Abstracts for IV All-Union Conference on Plasma Accelerators and Ion Injectors*, Moscow, 1978, pp. 23-24.
- <sup>28</sup>Garkusha, V. I., Yerofeyev, V. S., Lyapin, Ye. A., and Chugina, S. P., "Characteristics of a Single-Stage Cesium Anode-Layer Accelerator" (in Russian), *Abstracts for IV All-Union Conference on Plasma Accelerators and Ion Injectors*, Moscow, 1978, pp. 25-26.
- <sup>29</sup>Yerofeyev, V. S. and Safronov, I. N., "Operational Characteristics of a Double-Stage Cesium Anode-Layer Accelerator" (in Russian), *Abstracts for IV All-Union Conference on Plasma Accelerators and Ion Injectors*, Moscow, 1978, pp. 27-28.
- <sup>30</sup>Mironov, O. N., "Investigations of the Operation of a Cesium Accelerating Stage in a Double-Stage Anode-Layer Accelerator" (in Russian), *Abstracts for IV All-Union Conference on Plasma Accelerators and Ion Injectors*, Moscow, 1978, pp. 29-30.
- <sup>31</sup>Antipov, A. T., Grishkevich, A. D., Ignatenko, V. V., Kapulkin, A. M., Prisyakov, V. F., and Statsenko, V. V., "Double-Stage Closed Electron Drift Accelerator" (in Russian), *Abstracts for IV All-Union Conference on Plasma Accelerators and Ion Injectors*, Moscow, 1978, pp. 66-67.
- <sup>32</sup>Bardadymov, N. A., Ivashkin, A. B., Leskov, L. V., and Trofimov, A. V., "Hybrid Closed Electron Drift Accelerator" (in Russian), *Abstracts for IV All-Union Conference on Plasma Accelerators and Ion Injectors*, Moscow, 1978, pp. 68-69.
- <sup>33</sup>Morozov, A. I., *Physical Principles of Cosmic Electro-Jet Engines, Vol. I*, (in Russian), Atomizdat, Moscow, 1978, pp. 8-16.
- <sup>34</sup>Shadov, V. P., Porotnikov, A. A., Rilov, U. P., and Kim, V. P., "Plasma Propulsion Systems: Present State and Development," 30th International Astronautical Congress, Sept. 1979.
- <sup>35</sup>Knauer, W., "Mechanism of the Penning Discharge at Low Pressures," *Journal of Applied Physics*, Vol. 33, June 1962, pp. 2093-2099.
- <sup>36</sup>Knauer, W. and Lutz, M. A., "Measurement of the Radial Field Distribution in a Penning Discharge by Means of the Stark Effect," *Applied Physics Letters*, Vol. 2, March 1963, pp. 109-111.
- <sup>37</sup>Dow, D. G., "Electron-Beam Probing of a Penning Discharge," *Journal of Applied Physics*, Vol. 34, Aug. 1963, pp. 2395-2400.
- <sup>38</sup>Knauer, W., Fafarman, A., and Poeschel, R. L., "Instability of Plasma Sheath Rotation and Associated Microwave Generation in a Penning Discharge," *Applied Physics Letters*, Vol. 3, Oct. 1963, pp. 111-112.
- <sup>39</sup>Kervalishvili, N. A. and Zharinov, A. V., "Characteristics of a Low-Pressure Discharge in a Transverse Magnetic Field," *Soviet Physics-Technical Physics*, Vol. 10, June 1966, pp. 1682-1687.
- <sup>40</sup>Popov, Yu. S., "Low-Pressure Cold-Cathode Penning Discharge," *Soviet Physics-Technical Physics*, Vol. 12, July 1967, pp. 81-86.
- <sup>41</sup>Kervalishvili, N. A., "Effect of Anode Orientation on the Characteristics of a Low-Pressure Discharge in a Transverse Magnetic Field," *Soviet Physics-Technical Physics*, Vol. 13, Oct. 1968, pp. 476-482.
- <sup>42</sup>Kervalishvili, N. A., "Instabilities of a Low-Pressure Discharge in a Transverse Magnetic Field," *Soviet Physics-Technical Physics*, Vol. 13, Oct. 1968, pp. 580-582.
- <sup>43</sup>Smirnikskaya, G. V. and Nguen, K. T., "The Center Potential and Electron Density in a Penning Discharge," *Soviet Physics-Technical Physics*, Vol. 14, Dec. 1969, pp. 783-788.
- <sup>44</sup>Reikhrudel', E. M., Smirnikskaya, G. V., and Nguen, K. T., "Dependence of Current on Parameters in a Penning Discharge," *Soviet Physics-Technical Physics*, Vol. 14, Dec. 1969, pp. 789-795.
- <sup>45</sup>Popov, Yu. S., "Anode Sheath in a Strong Transverse Magnetic Field," *Soviet Physics-Technical Physics*, Vol. 15, Feb. 1971, pp. 1311-1315.
- <sup>46</sup>Erofeev, V. S. and Sanochkin, Yu. V., "Ionization Instability of a Self-Sustaining Low-Pressure Discharge in a Strong Transverse Magnetic Field," *Soviet Physics-Technical Physics*, Vol. 15, March 1971, pp. 1413-1417.
- <sup>47</sup>Smirnikskaya, G. V. and Nosyrev, I. A., "Oscillations in a Low-Pressure Penning Discharge," *Soviet Physics-Technical Physics*, Vol. 15, May 1971, pp. 1832-1838.
- <sup>48</sup>Barkhudarov, E. M., Kervalishvili, N. A., and Kortkhondzhiya, V. P., "Anode Sheath Instability and High-Energy Electrons in a Low-Pressure Discharge in a Transverse Magnetic Field," *Soviet Physics-Technical Physics*, Vol. 17, March 1973, pp. 1526-1529.
- <sup>49</sup>Mukhamedov, R. F., "Similarity Criteria in the Penning Discharge," *Soviet Physics-Technical Physics*, Vol. 20, Sept. 1975, pp. 1254-1256.
- <sup>50</sup>Kaufman, H. R., "Theory of Ion Acceleration with Closed Electron Drift, AIAA Paper 82-1919, Nov. 1982.
- <sup>51</sup>Kaufman, H. R. and Robinson, R. S., "Plasma Processes in Inert-Gas Thrusters," *Journal of Spacecraft and Rockets*, Vol. 18, Sept./Oct. 1981, pp. 470-476.
- <sup>52</sup>Robinson, R. S. and Kaufman, H. R., "Ion Thruster Technology Applied to a 30-cm Multipole Sputtering Ion Source," *AIAA Journal*, Vol. 15, May 1977, pp. 702-706.
- <sup>53</sup>Robinson, R. S., "Physical Processes in Directed Ion Beam Sputtering," NASA CR-159567, March 1979, App. A.
- <sup>54</sup>Spitzer, L. Jr., *Physics of Fully Ionized Gases*, 2nd ed., Interscience Publishers, N. Y., 1962, pp. 47-48.
- <sup>55</sup>Chen, F. F., *Introduction to Plasma Physics*, Plenum Press, N. Y., 1974, p. 169.
- <sup>56</sup>Plank, G. M., Kaufman, H. R., and Robinson, R. S., "Experimental Investigations of a Hall-Current Accelerator," AIAA Paper 82-1920, Nov. 1982.
- <sup>57</sup>Wilhelm, H. E., "Anomalous Correlation and Diffusion in Microfields of Magnetoactive Plasmas," *Nuclear Technology/Fusion*, Vol. 3, Jan. 1983, pp. 144-148.
- <sup>58</sup>Kaufman, H. R., Robinson, R. S., and Frisa, L. E., "Ion Flow Experiments in a Multipole Discharge Chamber," AIAA Paper 82-1930, Nov. 1982.
- <sup>59</sup>Kaufman, H. R. and Robinson, R. S., "Ion Source Design for Industrial Applications," *AIAA Journal*, Vol. 20, June 1982, pp. 745-760.